ENHANCING UPLINK PERFORMANCE IN UTRAN LTE NETWORKS BY LOAD ADAPTIVE POWER CONTROL[1]

Robert Müllner, Carsten F. Ball, and Malek Boussif
Nokia Siemens Networks GmbH & Co. KG
Radio Access
Lise-Meitner-Str.7/2, D-89081 Ulm, Germany
{robert.muellner, carsten.ball}@nsn.com

Research Technology & Platforms
Niels Jernes vej 10, DK-9220 Aalborg, Denmark
malek.boussif@nsn.com

Johann Lienhart and Peter Hric
Siemens AG
Siemensstr. 92, A-1210 Vienna, Austria
{johann.lienhart, peter.hric}@siemens.com

Abstract — Uplink power control in 3GPP UTRAN Long Term Evolution (LTE) networks consists of a closed-loop scheme around an open-loop point of operation. The uplink performance of the network is decisively influenced by power control. This paper provides insight into the uplink power control procedure and its interworking with Adaptive Transmission Bandwidth (ATB) as well as Adaptive Modulation and Coding (AMC). A detailed performance evaluation is presented based on system level simulations. In the first step the performance of pure open-loop power control was analyzed and the impact of parameter settings on resource allocation, utilization of specific modulation and coding schemes, re-transmission rate, and resulting throughput was determined. A two-dimensional parameter optimization for full path-loss compensation and fractional power control was performed to conclude the best strategy for the trade-off between network capacity and coverage. In the second step the impact of traffic load on the interaction between the different LTE radio resource management algorithms was analyzed. A novel strategy is presented which introduces traffic load dependent decisions for the closed-loop power control component to optimize the uplink throughput. This solution provides an automatic configuration for LTE networks without further intervention by the operator.

Keywords — LTE, Uplink, Load Adaptive Power Control, Closed-Loop Power Control, Fractional Power Control.

1. INTRODUCTION

Mobile broadband access with high data rates and low latencies becomes reality with the deployment of UTRAN Long Term Evolution (LTE) standardized in 3GPP [1]-[9]. To achieve optimal network performance the role of Power Control (PC) becomes decisive for maintaining the required Signal over Interference plus Noise Ratio (SINR) according to Quality of Service (QoS) requirements while controlling at the same time the inter-cell interference [10]. Especially uplink (UL) PC is a means to effectively reduce interference in the network and to improve cell edge performance. This is of particular importance

[1] A previous version of this paper was presented in the 7th International Workshop on Multi-Carrier System & Solutions (MC-SS 2009), Herrsching, Germany

considering the fact that typical LTE deployments have a frequency reuse 1. This study gives insight into the behavior of the different types of UL PC such as fractional PC and full path-loss (PL) compensation as well as load adaptive PC. A full-blown system level simulation environment was used for this analysis. Focus was set on the investigation of the interworking between PC, Adaptive Transmission Bandwidth (ATB), and Adaptive Modulation and Coding (AMC). Based on this fundamental behavior the impact of traffic load on UL power controlled LTE networks was analyzed and a strategy was developed to optimize UL performance under various load conditions. The paper is structured as follows. Section 2 describes the UL PC algorithm. The simulation model is introduced in Section 3. Detailed simulation results are presented and discussed in Section 4. A novel strategy for adapting UL transmission power according to the instantaneous traffic load is introduced in Section 5 and its performance gain is quantified. Conclusions are given in Section 6.

2. UPLINK POWER CONTROL ALGORITHM

The LTE PC algorithm specified in [4] is based on a combination of an Open Loop (OL) and Closed Loop (CL) scheme. The User Equipment (UE) controls its output power such that the power per Resource Block (RB) is kept constant irrespective of the allocated transmission bandwidth. One RB is the lowest scheduling unit occupying a bandwidth of 180 kHz and a Transmission Time Interval (TTI) of 1 ms. As long as there is no PC command received from eNodeB on the Physical Downlink Control Channel (PDCCH), the UE exclusively performs OLPC based on PL estimates, broadcast system parameters and dedicated signaling. Whenever the UE receives a CLPC command from eNodeB via PDCCH the UE has to correct its transmission power if necessary. In general the transmission power for the Physical Uplink Shared Channel (PUSCH) is set by the UE according to

$$P = \min\{ P_{\max} , 10 \cdot \log_{10} M + P_0 + \alpha \cdot PL + \Delta_{TF} + \Delta_i \} . \qquad (1)$$

- P_{max} is the maximum allowed UE transmission power specified at 23 dBm (200 mW) for UE power class 3 [11]. P_{max} is a broadcasted parameter that can be also configured to a lower value than that defined by the UE power class.
- M is the bandwidth of the PUSCH resource assignment to a specific UE expressed in number of RBs.
- P_0 is the set-point comprising a cell specific and UE specific component [4] to define the target receive level.
- $\alpha \in \{0, 0.4, 0.5, 0.6, 0.7, 0.8, 0.9, 1\}$ is a broadcasted cell specific parameter defining the degree of PL compensation for fractional PC (FPC). The idea of classic OLPC schemes in the UL is that all UEs are received at the eNodeB with the same power spectral density, which is known as full PL compensation. In addition 3GPP introduced the so-called FPC [12]-[13], allowing users to operate at a lower receive signal level compared to that based on full PL compensation resulting in less interference generated to neighboring cells [10].
- PL is the downlink PL estimate calculated by the UE.
- Δ_{TF} is a Transport Format (TF) dependent offset [4] used to consider different SINR requirements for various Modulation and Coding Schemes (MCS).

- Δ_i represents the power correction value provided by CLPC. Optionally the correction can be either accumulative or absolute [4], which is signaled by the network. In this study the first option was investigated.

3. SIMULATION MODEL

A hexagonal regular cell layout in an urban deployment scenario with 500 m Inter Site Distance (ISD) and an available frequency spectrum of 10 MHz was simulated in frequency reuse 1. The deployment area comprises 21 cells placed in a wrap-around model assuming a Typical Urban (TU) channel model. A PL model for small cells with PL slope of 37.6 dB per decade was used. Additional penetration loss of 20 dB for indoor coverage was taken into consideration [14]. Basic configuration parameters such as PL model and antenna diagram were selected in accordance to [14].

The number of users within the simulation area of 21 cells was kept constant but the distribution of the users on cells was unbalanced. Slow moving subscribers were assumed. During the simulation run a UE can change its serving cell by handover based on a power budget decision criterion (handover margin 3 dB). A full (infinite) buffer traffic model proposed for LTE benchmark evaluation in [15] was assumed. The simulation model includes synchronous non-adaptive Hybrid Automatic Repeat Request (HARQ) with Chase Combining. The essential simulation parameters are listed in Table I.

TABLE I
Parameters of the System Level Simulation Model.

Parameter	Value
Layout	7 sites – 3 cells/site – wrap around
Propagation scenario	Macro 1 (ISD 500 m) [14]
System carrier frequency	2 GHz (according to [14] for case 1)
System bandwidth	10 MHz for UL
Frequency reuse scheme	Reuse 1, no fractional reuse or interference avoidance applied
Fast fading model	According to [17]
Indoor penetration loss	20 dB (according to [14])
Traffic model	Full buffer [15], geometric session lifetime distribution (mean value 30 s)
eNodeB receiver	2 RX (maximum ratio combining)
UE speed	3 km/h
Scheduler	Round robin, channel unaware scheduler, i.e. no frequency dependent scheduling (sounder disabled)
Adaptive Transmission Bandwidth (ATB)	Ideal (based on power headroom report without measurement error)
Link adaptation	Slow Adaptive Modulation and Coding (AMC), BLER target = 10 %
Modulation and Coding	QPSK [R=1/3, 1/2, 2/3], 16QAM [R=1/2, 2/3, 5/6], 64QAM [R=2/3, 5/6, 9/10]
Maximum UE transmission power P_{max}	23 dBm (200 mW) according to [11] for UE power class 3
Uplink power control	Open and closed-loop, Closed-loop PC interval = 50 ms
Δ_{TF}	0, i.e. transport format dependent offset disabled
Δ_i for closed-loop PC	{-1, 0, 1, 3} dB, accumulation enabled

3.1 Adaptive Modulation and Coding (AMC)

LTE supports in UL Quadrature Phase-Shift Keying (QPSK) and 16 Quadrature Amplitude Modulation (QAM), 64QAM is optional. Slow AMC [16] was assumed with update period of 30 ms for switching between MCS depending on radio conditions. Out of all available MCS according to 3GPP only three MCS per modulation type were selected: MCS-0 to 2 for QPSK, MCS-3 to 5 for 16QAM, and MCS-6 to 8 for 64QAM as listed in Table I.

3.2 Adaptive Transmission Bandwidth (ATB)

ATB is based on Power Headroom Reports (PHR) [4] and sets the number of allocated RBs according to available UL power and cell load. Adjustment of the bandwidth assigned to a specific UE by ATB is required whenever the PHR indicates that UE has still some transmission power reserve or in the other case that the UE runs out of power. For example a UE has an allocation of 10 UL RBs and PHR indicates +3 dB (power reserve), hence ATB extends upcoming allocation up to 20 RBs. On the other hand a PHR of -3 dB would limit upcoming allocation down to 5 UL RBs. ATB is necessary to avoid UE overheating and especially in case of lack of power to concentrate the remaining power on less RBs, thus allowing a regular data transmission in UL even at the cell edge. In the simulation model ATB is updated every TTI and was ideally modeled, i.e. assuming no measurement error.

4. SIMULATION RESULTS

4.1 Performance Analysis of Open-Loop Power Control

The impact of the power offset P_0 on the UL performance was analyzed assuming full PL compensation ($\alpha = 1$) and a mean number of ten UEs per cell. Fig. 1a shows the cumulative distribution function (CDF) of transmission power per RB for four different P_0 settings in the range from -120 dBm to -60 dBm. For low P_0 values (-120 dBm and -100 dBm) the total UL transmission power according to (1) is low and the transmission power per RB is not limited. For both P_0 settings the total UE transmission power (not shown here) is below P_{max} of 23 dBm and no UE power shortage was observed. In contrast, at higher power offset 17% of the RBs reach P_{max} for P_0 = -80 dBm, i.e. the requested transmission power according to (1) cannot be provided even for the allocation of a single RB only. For P_0 = -60 dBm limitation of transmission power per RB was observed for 76% of the RBs. Hence proper cell-specific setting of P_0 is essential, especially if pure OLPC is applied. If P_0 is set too high, not only UEs located at the cell border, but also those in the vicinity of the eNodeB use unnecessarily high transmission power reducing battery life-time and might get less bandwidth assigned by ATB.

The number of RBs assigned in UL to the UE depends on *(a)* availability of physical resources in the cell and *(b)* available power headroom. The CDF of the number of allocated RBs per UE and TTI is depicted in Fig. 1b. For P_0 = -120 dBm five or more RBs were assigned to the UE in 99.7% of the TTIs. A restriction in the number of assigned RBs is

purely related to the number of users simultaneously served in the cell and not to UL power constraints. Recall that the 50 RBs in 10 MHz are shared by 10 UEs per cell in average.

For P_0 = -100 dBm five or more RBs were assigned to the UE in 94% of the TTIs. Selecting higher P_0 results in a higher transmission power per RB and consequently leads to a reduction of the RBs assigned to the UE by ATB, because the total UE transmission power defined in (1) must not exceed P_{max}. For P_0 = -80 dBm only a single RB was assigned to the UE in 73% of the TTIs. For P_0 = -60 dBm the ratio of TTIs for which only a single RB was assigned to the UE is even 98%. Note that 10 UEs per cell with a single RB allocated per UE results in a fractional load of 20% only. Fig. 1b demonstrates the utilization of the deployed air interface resources depending on P_0 setting.

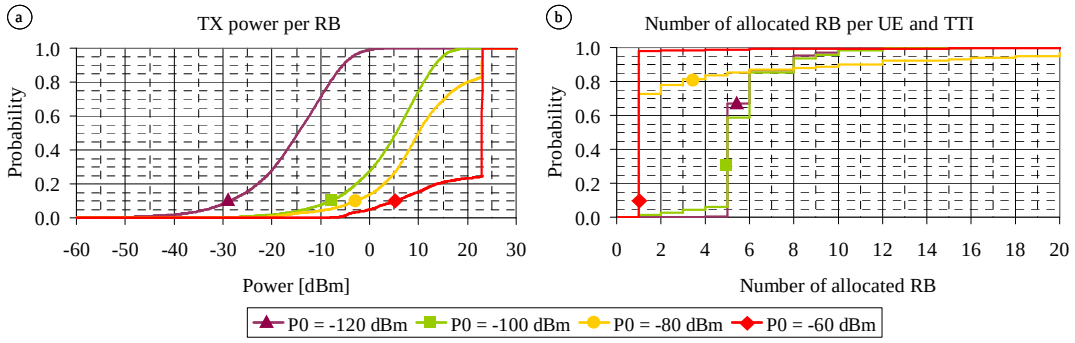

Figure 1. CDF of (a) transmission power per Resource Block and (b) number of allocated Resource Blocks per UE and TTI for α = 1 and various P_0 settings.

Transmission power per RB and number of assigned RBs have significant impact on the SINR as shown in Fig. 2a. In the fully loaded network using P_0 = -120 dBm only 13% of the bursts are received at a SINR of 1 dB or higher, corresponding to the operating point of the most robust MCS-0 used in this study (cf. Figure 2b). The SINR distribution gradually improves as P_0 increases to -100 dBm and -80 dBm. For P_0 = -60 dBm the high interference at a low number of allocated RBs (cf. Figure 1b) causes flattening of the SINR distribution, i.e. a considerable number of users enjoy high SINR, while other users suffer from low SINR resulting in a poor cell border throughput performance. Note that for P_0 = -60 dBm in most cases only one RB per UE was assigned, i.e. the SINR distribution reflects the quality on the sparse number of allocated resources only.

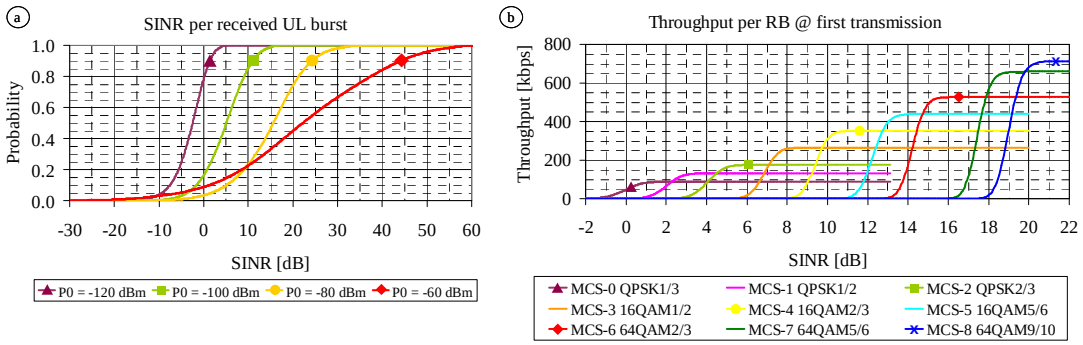

Figure 2. (a) CDF of Signal over Interference plus Noise Ratio per received uplink burst for α = 1 and various P_0

settings and (b) throughput[2] per Resource Block vs. Signal over Interference plus Noise Ratio (first transmission) for the applied modulation and coding schemes.

Fig. 2b shows the throughput per RB for the first transmission vs. SINR obtained from link level simulations. The operating range of QPSK modulation is 1 to 7 dB. For 16QAM a SINR of 7 to 15 dB is required. The operating point of 64QAM is 15 dB and higher.

The optimum MCS per UE depends on radio conditions and is selected by AMC based on link quality measurements. For P_0 = -120 dBm the resulting SINR (cf. Figure 2a) is typically too low for selecting a high MCS and hence MCS-0 dominates. The CDF of MCS level per allocated code word in Fig. 3a shows that for P_0 = -120 dBm almost 100% of the UEs use MCS-0. For P_0 = -100 dBm the ratio of MCS-0 utilization is 43%. For this P_0 setting still almost 100% QPSK utilization was observed. For P_0 = -80 dBm the SINR is substantially higher and hence the percentage of QPSK modulation is only 50%, while further 45% of the code words were transmitted in 16QAM. The ratio of 64QAM utilization is limited to 5%. In contrast for P_0 = -60 dBm a 64QAM utilization of 25% was determined.

UE throughput is also affected by the percentage of cell resources utilized for re-transmissions. Fig. 3b shows the CDF of RBs per TTI used for re-transmission of erroneous code words. For 50% of the TTIs 24 out of 50 available RBs in the cell were occupied for re-transmissions using P_0 = -120 dBm. Note that the block error rate (BLER) target of 10% is not maintained. For P_0 = -100 dBm only 10% of the RBs (i.e. 5 RBs) are used with 50% probability for re-transmissions. This number amounts 1 RB for P_0 = -80 dBm and -60 dBm, i.e. re-transmission gets more or less negligible.

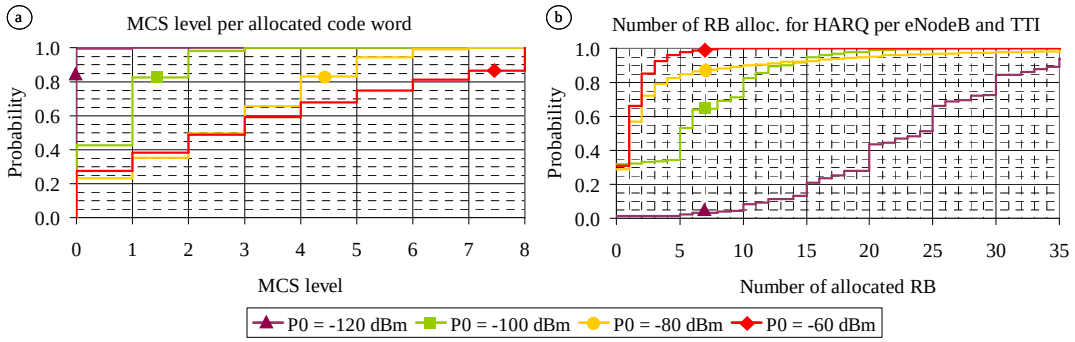

Figure 3. CDF of (a) Modulation and Coding Scheme utilization and (b) number of Resource Blocks allocated for HARQ for α = 1 and various P_0 settings.

The CDF of the resulting cell throughput is shown in Fig. 4a. Note that cell throughput is an indicator for spectrum efficiency and system capacity. Poor throughput (low capacity) was obtained in the two extreme cases, P_0 = -120 dBm with a mean value of 1969 kbps and P_0 = -60 dBm with 3309 kbps, respectively. The major reason in the first case is the low transmission power resulting in a high number of assigned RBs but low SINR. Consequently only the most robust MCS was applied combined with a high re-transmission rate. The reason for the low throughput obtained for P_0 = -60 dBm is the high transmission power per RB resulting for full PL compensation in a resource assignment mostly restricted to a single RB. Although high MCS were selected due to the high SINR the resulting cell throughput is

[2] The link level files for the 9 MCS used in this series of simulations are related to an early phase of standardization of LTE with a different physical layer. This impacts the absolute values of the shown throughputs by around 8%.

poor due to fractional loading. The mean cell throughput was improved to 7830 kbps by choosing P_0 = -80 dBm.

The performance of individual connections was applied as further criterion. The active session throughput is defined as the average throughput per session during active data transfer, shown in Fig. 4b.

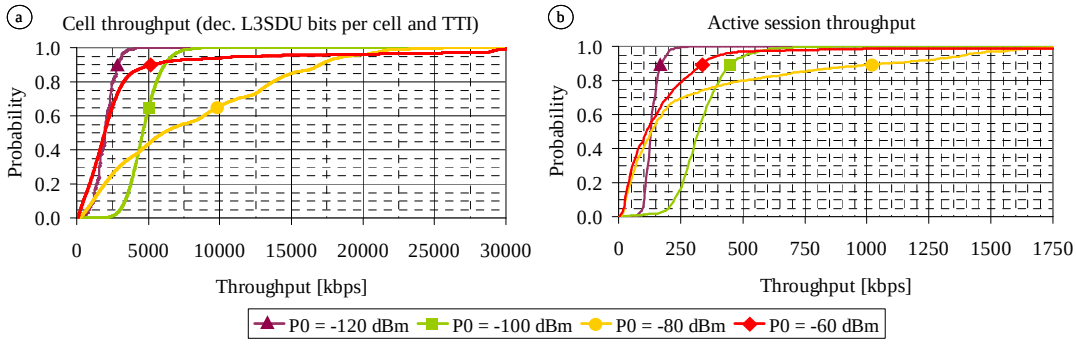

Figure 4. CDF of (a) cell throughput and (b) user throughput for $\alpha = 1$ and various P_0 settings.

This analysis demonstrated the impact of OLPC P_0 settings on UE and cell throughput. A strong conjunction between PC, RB assignment by ATB, MCS selection handled by AMC and re-transmission rate was observed.

4.2 Joint P_0 and α Optimization

For analyzing the impact of fractional PC ($\alpha < 1$) a two-dimensional optimization with respect to UE and cell throughput was performed for P_0 ranging from -120 dBm to -10 dBm and $\alpha \in \{0, 0.4, 0.5, 0.6, 0.7, 0.8, 0.9, 1\}$. The average traffic load was kept at ten UEs per cell. Fig. 5a shows the mean cell throughput, which is a measure for the network capacity. The 5th percentile active session throughput, which is used as measure for coverage, is shown in Fig. 5b.

For full PL compensation ($\alpha = 1$) the highest mean cell throughput of 8213 kbps was achieved for P_0 = -82 dBm. However, the 5th percentile active session throughput shows poor 19 kbps. The latter value reaches its maximum of 206 kbps at P_0 = -106 dBm. In case of FPC a maximum cell throughput of 8738 kbps was achieved for $\alpha = 0.7$ and P_0 = -52 dBm. For this combination the 5th percentile active session throughput reveals unacceptable 15 kbps. At constant P_0 a further decrease of α below 0.7 results in improved coverage but reduced capacity.

Note that only a small range of reasonable P_0 and α settings is feasible (small stripe), which are not fully correlated for cell (cf. Figure 5a) and 5th percentile UE throughput (cf. Figure 5b).

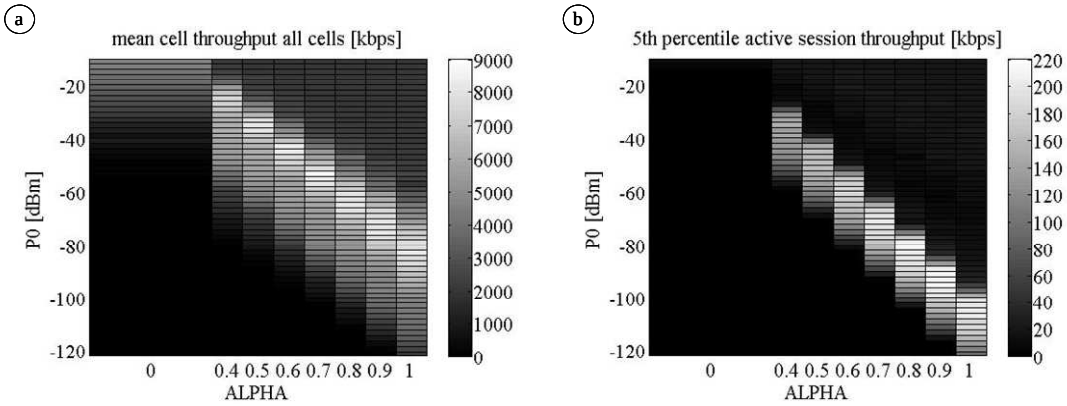

Figure 5. (a) Mean cell throughput and (b) 5th percentile active session throughput depending on α and P_0.

Fig. 6 shows the trade-off between capacity and coverage. For full PL compensation (α = 1) a good compromise is achieved for -106 dBm ≤ P_0 ≤ -100 dBm, for FPC the combination of P_0 = -80 dBm and α = 0.8 provides good results. In this optimization process focus was set on achieving high coverage at competitive capacity. The gradient of the performance curves in Fig. 6 is high and targeting at higher cell throughput always leads to user throughput degradation, i.e. any increase of P_0 beyond the recommended values would slightly increase the mean cell throughput but significantly reduce the 5th percentile user throughput. The percentage of loss in coverage would exceed the percentage of gain in capacity.

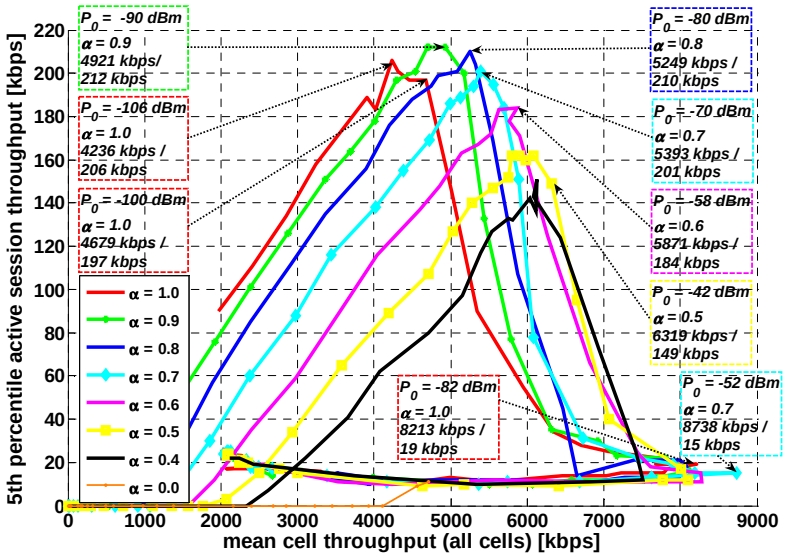

Figure 6. Trade-off between capacity and coverage for various α and P_0 settings.

4.3 Impact of Traffic Load on the Interworking between ATB, AMC and UL PC

The analysis in Section 4.1 demonstrated the different options for the distribution of the total transmission power P of the UE. Depending on the setting of P_0 the transmission power

can be distributed over many RBs resulting in low SINR, low MCS-level and consequently low number of transmitted user bits per RB. It can also be distributed over a low number of RB with high SINR, high MCS-level and high throughput per RB. The UL PC algorithm offers full flexibility for defining the strategy either by the selection of P_0 values or alternatively by adapting the transmission power via closed-loop power correction commands.

For determining the impact of traffic load on the interworking between ATB, AMC, and PC and identifying the optimum total UL transmission power at given load, the total UL transmission power P in (1) was adapted by a variation of the parameter P_0 in the range from -120 dBm to -60 dBm, while α in (1) was kept constant at 1. The simulated traffic load in the network was varied between 2 and 1050 UEs resulting in an average number of UEs per cell of 0.1 to 50. Fig. 7a shows the resulting mean cell throughput. The following conclusions are drawn:

- At very low traffic load with less than one UE per cell in average, highest capacity is achieved by P_0 around -100 dBm. At considerable low interference in the network this set-point is sufficiently high to avoid high re-transmission rate. At the considered load condition sufficient physical resources are available in the cell and the throughput is limited mainly by UL power constraints. Although SINR and MCS-level are low on the allocated RBs, the assignment of a high number of RB provides optimum capacity. Using low total transmission power at low load allows taking benefit from code gain in turbo codes by distributing the transmission power over multiple RBs.
- With increasing traffic load and distribution of the cell resources among multiple UEs served in the cell, more and more emphasis is placed to traffic load as the limiting factor for throughput. The resources of the cell are distributed among the registered UEs and UL transmission power constraints become less important for the lower number of RBs assigned per UE. Higher transmission power per RB leads to improved link quality. Fig. 7a shows that for a mean number of one to ten UEs per cell, P_0 has to be adapted from the value -92 dBm to -82 dBm to optimize capacity. Since the bandwidth assigned to each individual UE is limited by scheduling decisions, highest capacity is achieved by concentrating the transmission power on the few assigned RBs.
- Higher traffic load leads to an increase of interference in the network. As a consequence the quality on the radio channel is reduced leading to lower MCS-levels and throughput. The turn-over point is reached at a load of 10-20 UEs per cell. For higher traffic load a slight reduction of the total transmission power improves the cell capacity.

For the simulated traffic load, the range of transmission power adaptation required for capacity optimization covers 18 dB.

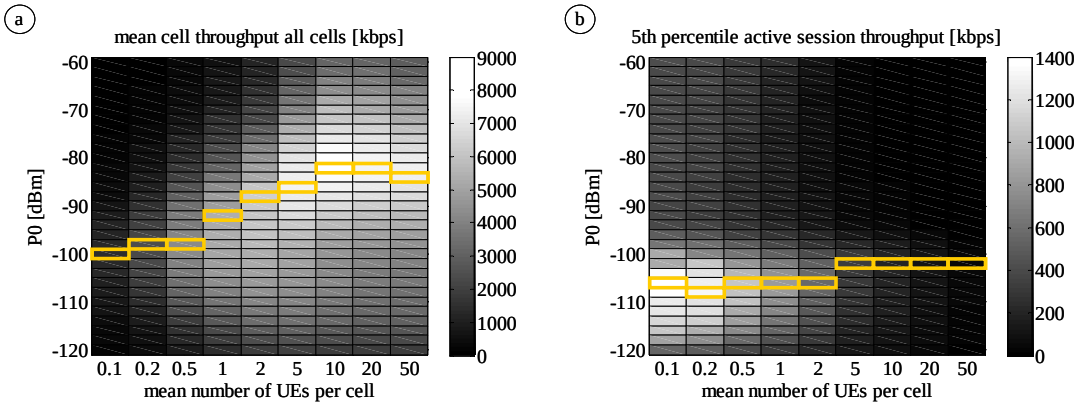

Figure 7. (a) Mean cell throughput depending on traffic load and P_0 and (b) 5th percentile active session throughput. Rectangles indicate P_0 settings to achieve highest throughput at given load.

Focus is now shifted from capacity to coverage analysis. Fig. 7b shows the 5th percentile active session throughput. The range of best suited P_0 for coverage optimization is lower in comparison to that necessary for capacity optimization and varies from -108 dBm to -102 dBm. Yet the trend of optimum P_0 as a function of traffic load observed for capacity optimization is preserved for coverage optimization. Low P_0 is beneficial for low traffic load situations, whereas an increase of the total transmission power provides advantages in high traffic load situations. Optimized P_0 as a function of traffic load differs for capacity and coverage optimization and must be aligned to achieve a compromise in network performance.

5. LOAD ADAPTIVE UPLINK POWER CONTROL

In Section 4.3 the impact of traffic load on the interaction of the relevant radio resource management algorithms PC, ATB, and AMC was analyzed. As traffic load in real networks heavily varies between cells and in time, the goal is the dynamic adaptation of the total transmission power P in (1) at different load situations without intervention of the network operator. Its impact on cell and user throughput was demonstrated in Fig. 7 by a variation of P_0. Fast adaptation of P_0 via System Information Broadcast or dedicated signaling, however, has some performance impacts. Instead of a dynamic adaptation of P_0 the total transmission power P used by the UE according to (1) can also be adjusted via closed-loop correction values Δ_i. These TPC commands calculated by the eNodeB and sent to the UE via PDCCH [4] allow frequent changes of the total transmission power at a large dynamic range using accumulation.

The method by which the closed-loop correction values Δ_i are generated is not standardized, hence a variety of algorithms are feasible for implementation. In this study two different strategies are compared. In the first strategy Δ_i values are triggered by evaluation of the traffic load, while in the second strategy this criterion was used to adapt a two-dimensional radio condition based decision matrix according to the instantaneous traffic load. The decision matrix compares filtered Received Signal Strength Indicator (RSSI) as indicator of the received level and SINR measurements as indicator of the received quality with configurable thresholds. These thresholds are controlled by traffic load decisions.

5.1 Closed-Loop Power Control Commands triggered by Load Conditions

This strategy uses traffic load as single criterion to trigger power corrections via the fast closed-loop component. The fundamental difference to the strategy proposed in Section 5.2 is that power corrections are not biased by SINR or RSSI measurements. Trigger condition is the number of registered users in the serving cell. Especially for bursty traffic further trigger criteria taking into consideration the bandwidth assigned to the UEs shall be applied, e.g. the RB utilization or noise rise. For services with specific QoS requirements the sum of weighting factors can be used as trigger condition.

At initial context setup the UE uses the static P_0 settings defined by system information broadcast and dedicated signaling. The difference between this static P_0 value and the target P_0 is calculated and continuously updated by the eNodeB. TPC commands for Δ_i = {-1, 0, 1, 3} dB are sent to the UE to minimize this difference and a virtual adaptive P_0 parameter is introduced in eNodeB to add accumulated Δ_i to the static P_0 value. A CLPC update interval of 50 ms was assumed. Two different vectors of target P_0 values were used for capacity optimization based on the results shown in Fig. 7a and coverage optimization according to Fig. 7b.

The performance of the Load Adaptive Power Control (LAPC) algorithm in comparison to static P_0 settings is demonstrated in Fig. 8. LAPC follows the upper envelope of the best performing static P_0 setting from 1 to 100 UEs per cell, i.e. the proposed algorithm proves its ability to adapt UL transmission power to the prevailing traffic load and offers an automatically configuring system for which no further intervention by the operator is necessary. The range of 0.1 to 1 UEs per cell in average is of statistical interest only. The eNodeB serves either zero, one, or more UEs. Nevertheless, a combination of the applied number of registered users criterion with noise rise allows to consider also the interference generated in the neighboring cells for triggering power corrections. A cluster shall be defined and the defensive strategy of considering only traffic load in the serving cell can be extended to the surrounding cells. This extension could be used to further improve the LAPC performance in the range of less than one UE per cell in average.

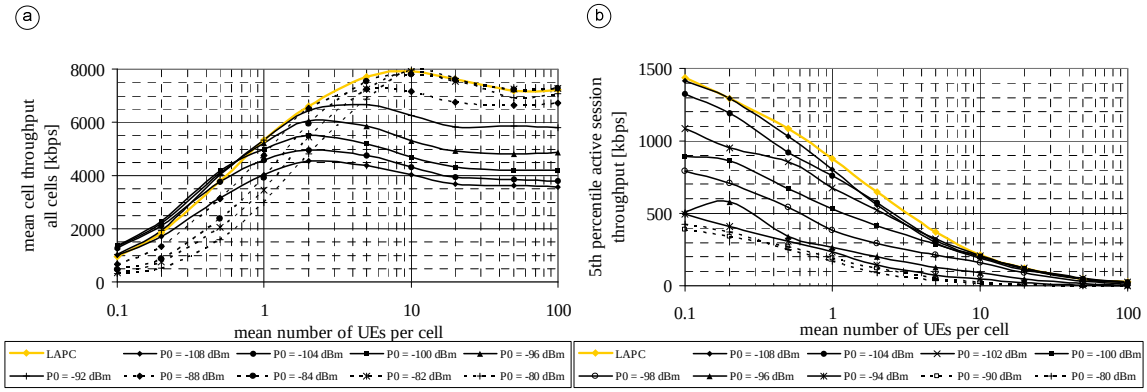

Figure 8. (a) Mean cell throughput depending on traffic load and (b) 5th percentile active session throughput for LAPC vs. static P_0 settings.

Fig. 8b demonstrates the excellent performance of LAPC for coverage optimization using a vector of target P_0 values according to the simulation results shown in Fig. 7b. Between these two extreme cases, i.e. pure capacity driven and pure coverage driven

throughput optimization any compromise can be selected by defining the target P_0 vector as a trade-off between capacity and coverage.

5.2 Combined Radio Condition and Load dependent Trigger Criteria

The original intention of the closed-loop component is to compare measurements on the receiver side with target values and to command power corrections to the transmitter, if necessary. A specific implementation is described in [18], where closed-loop correction values Δ_i are determined by comparing filtered Received Signal Strength Indicator (RSSI) and SINR measurements with configurable thresholds representing a two-dimensional decision matrix as shown in Fig. 9a. The lower/upper SINR and RSSI thresholds LOW_QUAL, UP_QUAL, LOW_LEV, and UP_LEV define a so called PC window. $\Delta_i = 0$ dB is commanded to the UE if filtered measurements of SINR and RSSI are well within the PC window (quadrant 5). Power decrease by $\Delta_i = -1$ dB is commanded if both components (quadrant 3) or one of them exceeds the PC window while the other one does not fall below the lower threshold (quadrant 2 and 6). If the filtered measurements of at least one of the components fall below the PC window, power increase $\Delta_i = +1$ dB or $\Delta_i = +3$ dB, respectively, is commanded, depending on the deviation of filter outputs from lower thresholds.

In this second LAPC strategy the PC window is shifted by a load dependent adaptation of the thresholds. The deviation between static and target P_0 was continuously calculated. Instead of triggering load dependent TPC commands, the SINR and RSSI thresholds were increased or decreased by the calculated deviation. For a difference of -3 dB the SINR and RSSI thresholds were decreased by the same value. In consequence lower quality and level requirements were applied resulting in TPC commands to adapt transmission power to the lower targets. The closed-loop decision matrix is now controlled by the prevailing radio conditions defined by SINR and RSSI, as well as traffic load as shown in Fig. 9b.

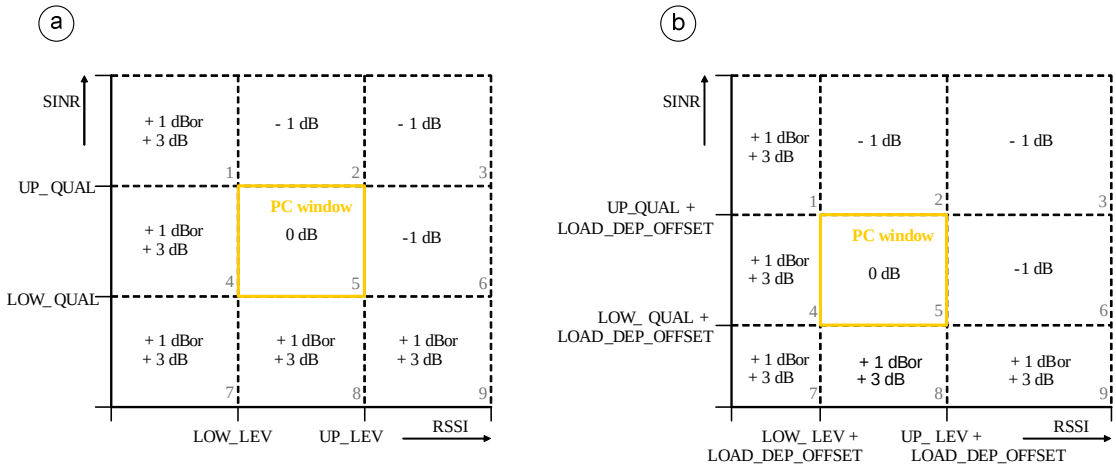

Figure 9. (a) Receive quality and level based closed-loop power control decision matrix and (b) its extension by traffic load decision criteria.

The different behavior of the CL component is demonstrated in the RSSI/SINR plot in Fig. 10 for a simulated average traffic load of two UEs per cell. Each point characterizes a

tuple of filtered RSSI and SINR values used for the decision on CLPC corrections of {-1, 0, 1, 3} dB. The blue rectangle defines the PC window initially configured for medium quality targets of SINR = [9; 12] dB and RSSI = [-96; -91] dBm. Green color indicates areas in which power increase by 1 dB was commanded, while the red cloud represents areas of power increase by 3 dB. Areas of power decrease by 1 dB are characterized by violet color. While clear borders between the different regions were observed for static PC thresholds in Fig. 10a, blurring of the edges occurred in Fig. 10b due to the dynamic adaptation of the thresholds.

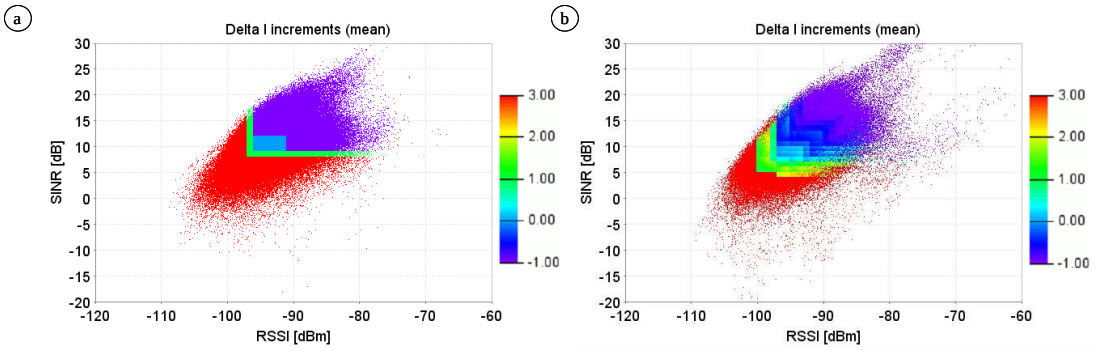

Figure 10. Closed-loop power control corrections in the RSSI/SINR plane featuring (a) clear borders between commanded Δ_i correction values and (b) blurred edges due to dynamic adaptation of the SINR/RSSI thresholds.

Both strategies, pure load-dependent generation of UL power corrections as well as adapting the thresholds of the closed-loop power control window can be applied to consider the traffic load dependence in the interworking between UL PC, ATB and AMC for throughput optimization.

6. CONLUSIONS

In this paper a detailed study of uplink power control performance in LTE networks was presented. Insight is given into the interworking between ATB, AMC, and power control. The impact of P_0 on open-loop power control assuming full path-loss compensation ($\alpha = 1$) was analyzed thoroughly. For P_0 ranging from -106 dBm to -100 dBm a good performance compromise in terms of capacity and coverage was found. For lower P_0 settings both capacity and coverage degrade due to low transmission power causing poor SINR, robust modulation and coding scheme selection with low throughput and high re-transmission rate. An increase of P_0 beyond -100 dBm leads to increase in capacity but at the same time to drastic coverage degradations. Using even higher P_0 results in fractional loading since ATB restricts the UE resource block allocation. For fractional power control ($\alpha < 1$) the combination of P_0 = -80 dBm and $\alpha = 0.8$ is recommended as a good compromise between capacity and coverage. Higher capacity was achieved by decreasing α, however, implying poor cell border performance at the same time.

The impact of traffic load on the interaction between ATB, AMC, and power control was analyzed and the best suited power offset for various traffic load was identified. The mechanism of the closed-loop PC component was used to dynamically adapt the static power offset P_0 to this load dependent target P_0. The result was an automatically configuring system to optimize throughput without any further operator intervention. Two different

strategies were analyzed. The first strategy uses the closed-loop component as fast mechanism to command uplink power corrections to the UE based on traffic load decisions and unbiased by quality and level targets. The second strategy combines load decisions with receive level and quality targets.

Both open-loop and closed-loop power control components offer high capabilities to tune the UL performance to achieve highest capacity, optimized cell border performance or a trade-off between both. In combination both components provide a powerful means for uplink power control in UTRAN LTE networks.

REFERENCES

[1] H. Holma, A. Toskala. *LTE for UMTS – OFDMA and SC-FDMA Based Radio Access*. John Wiley & Sons, 2009.

[2] 3GPP TS 36.211. Evolved Universal Terrestrial Radio Access (E-UTRA); Physical Channels and Modulation (Release 8), September 2009.

[3] 3GPP TS 36.212. Evolved Universal Terrestrial Radio Access (E-UTRA); Multiplexing and channel coding (Release 8), May 2009.

[4] 3GPP TS 36.213. Evolved Universal Terrestrial Radio Access (E-UTRA); Physical layer procedures (Release 8), September 2009.

[5] 3GPP TS 36.214. Evolved Universal Terrestrial Radio Access (E-UTRA); Physical layer – Measurements (Release 8), September 2009.

[6] 3GPP TS 36.321. Evolved Universal Terrestrial Radio Access (E-UTRA); Medium Access Control (MAC) protocol specification (Release 9), September 2009.

[7] 3GPP TS 36.331. Evolved Universal Terrestrial Radio Access (E-UTRA); Radio Resource Control (RRC); Protocol specification (Release 9), September 2009.

[8] 3GPP TS 36.300. Evolved Universal Terrestrial Radio Access (E-UTRA) and Evolved Universal Terrestrial Radio Access Network (E-UTRAN); Overall description (Release 9), September 2009.

[9] C. F. Ball, T. Hindelang, I. Kambourov, S. Eder. Spectral Efficiency Assessment and Radio Performance Comparison between LTE and WiMAX. In Proceedings *19th Annual IEEE International Symposium on Personal, Indoor and Mobile Radio Communications (PIMRC 2008), Cannes*, 2008.

[10] C. Úbeda Castellanos, D. López Villa, C. Rosa, K. I. Pedersen, F. D. Calabrese, P.-H. Michaelsen, J. Michel. Performance of Uplink Fractional Power Control in UTRAN LTE. In Proceedings *IEEE VTC Spring 2008, Beijing*, 2008.

[11] 3GPP TS 36.101. Evolved Universal Terrestrial Radio Access (E-UTRA); User Equipment (UE) radio transmission and reception (Release 9), September 2009.

[12] R1-073224. Way Forward on Power Control of PUSCH. 3GPP TSG RAN WG1 49bis, June 2007.

[13] M. Boussif, N. Quintero, F. D. Calabrese, C. Rosa, J. Wigard. Interference Based Power Control Performance in LTE Uplink. In Proceedings *International Symposium on Wireless Communication Systems 2008, Reykjavik*, 2008.

[14] 3GPP TR 25.814 Annex A. Physical layer aspects for evolved Universal Terrestrial Radio Access (UTRA) (Release 7), September 2006.

[15] R1-070674. LTE physical layer framework for performance verification. 3GPP TSG RAN1 48, February 2007.

[16] C. F. Ball, K. Ivanov, R. Müllner. A BLER based UL LTE AMC featuring Fast Upgrade and Emergency Downgrade. In Proceedings *ICT–MobileSummit 2008, Stockholm*, 2008.

[17] ETSI TR 101 112. 1998. Selection procedures for the choice of radio transmission technologies of the UMTS (UMTS30.03), April 1998.

[18] R. Müllner, C. F. Ball, K. Ivanov, J. Lienhart, P. Hric. *Contrasting Open-Loop and Closed-Loop Power Control Performance in UTRAN LTE Uplink by UE Trace Analysis. In Proceedings IEEE International Conference on Communications (IEEE ICC), Dresden*, 2009.